

**Probabilistic
regional sea-level
projections**

M. Perrette et al.

Title Page

Abstract

Introduction

Conclusions

References

Tables

Figures



Back

Close

Full Screen / Esc

Printer-friendly Version

Interactive Discussion



This discussion paper is/has been under review for the journal Earth System Dynamics (ESD). Please refer to the corresponding final paper in ESD if available.

Probabilistic projection of sea-level change along the world's coastlines

M. Perrette¹, F. Landerer², R. Riva³, K. Frieler¹, and M. Meinshausen¹

¹Potsdam Institute for Climate Impact Research (PIK) Telegraphenberg A26,
14412 Potsdam, Germany

²Jet Propulsion Laboratory/California Institute of Technology, Pasadena, USA

³Dept. Geoscience and Remote Sensing, Delft University of Technology,
Delft, The Netherlands

Received: 17 April 2012 – Accepted: 17 April 2012 – Published: 23 April 2012

Correspondence to: M. Perrette (mahe.perrette@pik-potsdam.de)

Published by Copernicus Publications on behalf of the European Geosciences Union.

Abstract

Climate change causes global mean sea level to rise due to thermal expansion of sea-water and loss of land ice from mountain glaciers, ice caps and ice-sheets. Locally, sea-level changes can strongly deviate from the global mean due to ocean dynamics. In addition, gravitational adjustments redistribute seawater away from shrinking ice masses, an effect currently not incorporated in climate models. Here, we provide probabilistic projections of sea level changes along the world's coastlines for the end of the 21st century under the new RCP emission scenarios, taking into account uncertainties across the cause-effect chain from greenhouse-gas emissions to ocean heat uptake and regional land-ice melt. At low latitudes, especially in the Indian Ocean and Western Pacific, sea level will likely rise more than the global mean (mostly by 10–20%, but up to 45 % in Tokyo area). Around the North Atlantic and the North-Eastern Pacific coasts, sea level will rise less than the global average or, in some rare cases, even fall. Our probabilistic regional sea level projections provide an improved basis for coastal impact analysis and infrastructure planning for adaptation to climate change.

1 Introduction

The current understanding of sea-level rise (SLR) remains incomplete as manifested by the inability to close the 20th century sea-level budget in the last IPCC report (Bindoff et al., 2007), as well as by the large uncertainty in 21st century projections (Lowe and Gregory, 2010; Rahmstorf, 2010). Current process-based projections can constrain ocean thermal expansion and the retreat of mountain glaciers and ice caps (MGIC). Simulations of the Greenland and Antarctic ice-sheets (GIS and AIS), however, are typically reduced to their surface mass balance (SMB) while neglecting fast ice dynamics (Gregory and Huybrechts, 2006; Meehl et al., 2007a). At the regional level, changes in the ocean dynamics and density structure due to water temperature and salinity changes (so-called steric changes) have a significant effect (Landerer et al.,

ESDD

3, 357–389, 2012

Probabilistic regional sea-level projections

M. Perrette et al.

Title Page

Abstract

Introduction

Conclusions

References

Tables

Figures



Back

Close

Full Screen / Esc

Printer-friendly Version

Interactive Discussion



Probabilistic regional sea-level projections

M. Perrette et al.

Title Page

Abstract

Introduction

Conclusions

References

Tables

Figures



Back

Close

Full Screen / Esc

Printer-friendly Version

Interactive Discussion



2007; Pardaens et al., 2010; Yin et al., 2009, 2010). The projected regional distribution of steric SLR is highly non-uniform, and deviations from the global mean may be of the same order of magnitude as the global thermal expansion (Yin et al., 2009). Large uncertainties remain in the simulated spatial SLR patterns, which vary greatly across the range of current coupled climate models (GCMs) (Pardaens et al., 2010). In addition to ocean dynamical changes, the melting and dynamic discharge of continental ice masses is accompanied by an instantaneous adjustment of the Earth's gravity field that causes water to migrate away from dwindling ice masses (Bamber and Riva, 2010; Clark and Lingle, 1977; Mitrovica et al., 2001). The Earth's shape and rotation vector are also affected and further modulate the pattern of sea-level changes. The land-ice influence on regional SLR hence depends on the spatial distribution of anticipated ice mass losses (Bamber and Riva, 2010; Clark and Lingle, 1977; Mitrovica et al., 2001). The number and complexity of the processes that influence regional SLR make it challenging to approach the problem in a comprehensive and consistent manner. In particular, gravitational patterns were long absent from syntheses such as the IPCC reports, and have received more attention only recently (Katsman et al., 2008; Slangen et al., 2011). Here, we present new estimates of regional SLR towards the end of the 21st century on a global domain and for the new Representative Concentration Pathways (RCPs) (Moss et al., 2010) in a probabilistic framework, combining the various SLR components and propagating the associated uncertainties.

2 Methods

By propagating uncertainties from future greenhouse-gas emissions to global and regional SLR, our approach provides an integrated uncertainty analysis – going beyond previous analyses of model ensembles for the SRES scenarios (Slangen et al., 2011). We use the reduced complexity carbon-cycle climate model MAGICC6 (Meinshausen et al., 2011) to constrain projections of hemispheric land and ocean temperatures and ocean heat uptake by their historical observations (Domingues, 2008; Brohan et al.,

2006), taking into account the range of uncertainty in natural and anthropogenic radiative forcing of the climate system as described in Meinshausen et al. (2009). Our projections are based on the new RCP scenarios, to be used in the next IPCC report to cover a broad range of future emissions. RCP8.5 is comparable with A1FI from IPCC AR4, while RCP4.5 and RCP6.0 resemble B1 and A1B, respectively (Moss et al., 2010).

Our general approach is to use probabilistic projections of the global mean contribution of each SLR component (Fig. 1e–h) to scale the associated spatial patterns (the so-called “fingerprints”; Fig. 1a–d). More specifically, we operate in a Monte Carlo framework to combine all uncertainties as described below.

2.1 Steric sea level

2.1.1 Global mean thermal expansion

The global mean ocean heat uptake is well simulated with the MAGICC6 model (Meinshausen et al., 2011, 2009), however at present the emulation of thermal expansion estimated from GCMs is not sufficiently accurate for the purposes of this study. In order to project global mean thermal expansion, we make use of the well-established quasi-linear relationship between global mean ocean heat uptake and thermal expansion as displayed in GCMs (Fig. S1a in the Supplement).

The slope of the relationship, or scaling coefficient, varies slightly among models, probably because of different depths of heat penetration into the ocean and differences in the background climatological temperature and salinity. These scaling coefficients were used to fit a Gaussian distribution (Fig. S1b in the Supplement). The distribution has a mean of $1.12 \times 10^{-25} \text{ mJ}^{-1}$ and a standard deviation of $0.12 \times 10^{-25} \text{ mJ}^{-1}$. Observation-based estimates typically get a number within the range $1.3\text{--}1.6 \times 10^{-25} \text{ mJ}^{-1}$, significantly larger than the GCMs (Domingues, 2008). The difference can most likely be reconciled considering the fact that the observational

Probabilistic regional sea-level projections

M. Perrette et al.

Title Page

Abstract

Introduction

Conclusions

References

Tables

Figures

◀

▶

◀

▶

Back

Close

Full Screen / Esc

Printer-friendly Version

Interactive Discussion



estimates are based on the top 700 m only, whereas our study concerns the whole water column (the expansivity of seawater is pressure dependent, decreasing with depth).

This Gaussian distribution for the scaling parameter (which derives thermal expansion from cumulative heat uptake) is then used in combination with probabilistic MAGICC6 results for heat uptake, a CMIP3 GCM quantity which MAGICC6 can closely emulate.

2.1.2 Dynamic sea-level changes

Regional variations of sea-level due to ocean density and circulation changes are based on 12 GCMs from the Coupled Model Intercomparison Project (CMIP3) (Meehl et al., 2007b). For each GCM, we derive a pattern of SLR with units of meters SLR per degree of global mean surface warming. These patterns are then randomly combined with MAGICC6 probabilistic global mean temperature (GMT) projections, and added on top of the global mean thermal expansion.

The selection of GCMs was based on data availability and on model skills at representing present-day dynamic sea-level (Yin et al., 2010). A spatial pattern of SLR for each model is derived by linear regression of dynamic sea-level changes against GMT under the SRES A1B scenario. The regression is performed over the 2000–2100 period, using yearly dynamic sea-level anomaly data with 1980–1999 as reference period. To yield regional SLR projections under the RCP scenarios, the regressed patterns are then randomly sampled (assuming each GCM pattern equally likely) and multiplied by MAGICC6's GMT projections.

We have confirmed that the linear regression explains most long-term changes during the 21st century. The derived patterns have relatively little inter-scenario variability as compared to the multi-model spread (Figs. S2–4, Table S1 in the Supplement).

Probabilistic regional sea-level projections

M. Perrette et al.

Title Page

Abstract

Introduction

Conclusions

References

Tables

Figures

◀

▶

◀

▶

Back

Close

Full Screen / Esc

Printer-friendly Version

Interactive Discussion



2.2 Mountain glaciers and ice caps

2.2.1 Global mean melt

The mountain glaciers and ice caps (MGIC) contribution (excluding those near the ice-sheets) is computed after Meehl et al. (2007a), itself based on Wigley and Raper (2005). It assumes a global SMB sensitivity, such that the rate of glacier's ice loss is proportional to a change in GMT, T as compared to pre-industrial equilibrium T_o . It also accounts for a decrease in global SMB sensitivity as the global glacier area decreases, assuming global volume-vs.-area scaling (Wigley and Raper, 2005):

$$\frac{dV_{gl}}{dt} = b_o (T - T_o) \left(1 - \frac{V_{gl}}{V_o} \right)^n \quad (1)$$

where b_o is the present (1961–2004 average) global SMB sensitivity, V_{gl} and V_o are the projected and present global glacier volumes (in sea level equivalent) respectively, and n is the scaling coefficient between global glacier area and volume, equal to 1.646. Other parameter values and their uncertainty ranges are indicated in Table 1. These are systematically sampled as part of our Monte Carlo approach.

The global SMB sensitivity b_o and the exponent n are the same as in the IPCC AR4 (Meehl et al., 2007a), while the total glacier volume V_o is taken from a more recent estimate (Radic and Hock, 2011). T_o is chosen consistently with Eq. (2) (see Sect. 2.3.1) and yields a 1961–2004 trend of $0.43 \pm 0.12 \text{ mm yr}^{-1}$, close to IPCC AR4's estimate (Lemke et al., 2007) ($0.43 \pm 0.15 \text{ mm yr}^{-1}$). We did not attempt to tune T_o with more up-to-date observational data since sensitivity tests showed that projections by 2100 are relatively insensitive to the precise specification.

In order to account for mountain glaciers present at the margin of the two main ice-sheets, we add, on top of MGIC contribution calculated from Eq. (1), another +21 % to the Antarctic Peninsula and +4 % to Greenland, based on a recent model projection (Radic and Hock, 2011).

Probabilistic regional sea-level projections

M. Perrette et al.

Title Page

Abstract

Introduction

Conclusions

References

Tables

Figures



Back

Close

Full Screen / Esc

Printer-friendly Version

Interactive Discussion



2.2.2 Spatial distribution of MGIC melt

The spatial pattern of sea-level rise induced by MGIC melt depends on the spatial distribution of the melt, and on corresponding gravitational adjustments. We account for gravitational effects by solving the sea-level equation with the same model as Bamber and Riva (2010). This approach includes self-gravitation, changes in Earth rotation, shoreline migration and elastic deformation of the solid Earth.

Our MGIC model (Eq. 1) only describes global MGIC melt, but we circumvent this limitation by assuming a fixed spatial distribution of the melt, based on a recent regionally-differentiated 21st century model projection (Radic and Hock, 2011, thereafter RH11). We therefore created a MGIC gravitational “fingerprint”, which describes the regional sea-level deviations in percent from the global mean MGIC contribution. The fingerprint is then scaled by the global MGIC contribution as calculated from Eq. (1), making use of the linear relationship between the specified melt distribution and the resulting spatial sea-level variations.

Our fingerprint aggregates the effect of glacier melt in 12 world regions, including the Antarctic Peninsula (Fig. 1b). The latter was attributed the whole Antarctic MGIC projections from RH11, ignoring potential contributions from around the margins of the East Antarctic where temperatures are expected to remain cold during the projection period. Note that we do not model the 7 regions of RH11 that are projected to individually cause less than 1 mm SLR by 2100, together accounting for about 1 % of the total MGIC contribution.

A comparison of our fingerprint with another fingerprint created from estimates of present-day MGIC melt helps to quantify the uncertainty arising from the spatial distribution of MGIC melt. Projected losses in RH11 for the Rocky Mountains and Western Canada are much less than present-day estimates (Figs. S5 and S6 in the Supplement), meaning possible overestimation of sea-level rise in these regions if the current rate is accurate and sustained (due to the underestimated contribution of both the gravitational drop of the sea surface and the elastic uplift of the solid Earth).

Probabilistic regional sea-level projections

M. Perrette et al.

Title Page

Abstract

Introduction

Conclusions

References

Tables

Figures



Back

Close

Full Screen / Esc

Printer-friendly Version

Interactive Discussion



Probabilistic regional sea-level projections

M. Perrette et al.

Title Page

Abstract

Introduction

Conclusions

References

Tables

Figures

◀

▶

◀

▶

Back

Close

Full Screen / Esc

Printer-friendly Version

Interactive Discussion



On the other hand, Iceland and Arctic Asia regions show large projected contribution to SLR whereas both current observations (Bamber and Riva, 2010, and references therein) and simulations of the past 1960–2000 period (RH11) indicate no significant contribution to global SLR (Fig. S6 in the Supplement). We interpret the latter as a robust indication of a likely increasing contribution from MGIC in northern high-latitude regions during the 21st century, which motivated our choice of using projected rather than present-day mass loss to generate the MGIC fingerprint.

2.3 Ice sheets

The potentially large, but uncertain, contributions by the two big ice sheets, on Greenland and Antarctica, warrants applying a range of approaches. Given the discrepancy between model simulations and current observations of ice-sheet mass changes (Rahmstorf, 2010; Rignot et al., 2011), there is at present little confidence in process-based projections of the ice sheets' response to warming, be it from surface warming, or from the surrounding ocean (Lowe and Gregory, 2010). In order to span the range of possible future evolution of the ice sheets, we consider three alternative approaches to compute global AIS and GIS contributions to SLR.

2.3.1 Top-down

The first approach is a “top-down” estimate, where global SLR projections are computed directly using a semi-empirical model (Rahmstorf et al., 2011) calibrated with past variations of observed global mean sea level and GMT. The GIS and AIS are then taken as the residual from total SLR projections after subtracting the steric and the MGIC contributions. Given the large uncertainty, we assume a simplified partitioning between GIS and AIS by varying the GIS/AIS loss ratio uniformly between 1/3 and 2/3 (Table 1). This is roughly consistent with recent observations (Bamber and Riva, 2010; Rignot et al., 2011), and turns out not to be critical for projected low- and mid-latitude SLR (see below, Fig. 6c).

Probabilistic regional sea-level projections

M. Perrette et al.

Title Page

Abstract

Introduction

Conclusions

References

Tables

Figures

◀

▶

◀

▶

Back

Close

Full Screen / Esc

Printer-friendly Version

Interactive Discussion



Semi-empirical methods are based on simple physical considerations and exploit the link between global mean sea-level and surface temperature (or radiative forcing) in the observational record, for projection of future SLR, with parameters calibrated with available observations (Grinsted et al., 2009; Rahmstorf, 2007; Vermeer and Rahmstorf, 2009). These methods typically yield future sea-level projections that can reach more than one metre of rise by 2100, which is significantly higher and in sharp contrast with the IPCC AR4 projections. One caveat in their application is that the semi-empirical relationships between temperature and sea-level variations is calibrated over a relatively narrow range of global mean temperature variation compared to the projected warming by 2100 (Lowe and Gregory, 2010), but in the absence of robust physical models that can reliably and explicitly simulate ice sheet response to warming based on first principles, semi-empirical methods still provide a useful, plausible alternative estimate (Rahmstorf, 2010).

In our “top-down” setting, global mean sea-level projections are computed after Rahmstorf et al. (2011), which is a slightly modified version of the Vermeer and Rahmstorf (2009) (henceforth called VR09) model, where the rate of sea-level change dH/dt is assumed to be proportional to the temperature anomaly relative to a pre-industrial equilibrium T_o . An additional term proportional to the derivative of global mean temperature dT/dt , captures the rapid response of sea-level to temperature variations, related to mixed-layer dynamics. Therefore:

$$\frac{dH}{dt} = a (T - T_o) + b \frac{dT}{dt} \quad (2)$$

where a and b are regression coefficients (see Table 1 for parameter values and their uncertainty ranges). Similar to VR09, sea-level time-series (Church and White, 2006) are corrected from artificial reservoir impoundment (building of dams) (Chao et al., 2008). Additionally, a recent ground-water mining correction (Konikow, 2011) is applied before the regression, so that we only account for climate-induced changes in sea-level.

The statistical approach is detailed in Rahmstorf et al. (2011), which accounts for autocorrelation in the residual time-series and the correlation between model parameters.

Here, we further inflate the projected uncertainty range by a factor of two to account for errors other than formal fitting of the model, such as data error and model choice. Furthermore, we do not extrapolate future groundwater pumping as is done in Rahmstorf et al. (2011).

2.3.2 Bottom-up I: IPCC AR4⁺

The second, alternative approach represents a low-end estimate of ice-sheet wastage, assuming IPCC AR4-like SLR contributions (referred to as IPCC AR4⁺) where only Greenland's surface mass balance contributes to the global mean SLR (Meehl et al., 2007a).

We randomly combined our 600 MAGICC6's GMT projections with 72 polynomial fits¹ of GIS's SMB as a function of GMT change (Gregory and Huybrechts, 2006). The polynomials were derived for the AR4 using various global and regional GCM simulations with a degree-day SMB model.

In AR4, it was assumed that Antarctica could also gain mass under global warming conditions due to an acceleration of the hydrological cycle and increased precipitation onto the ice sheet. Given recent observations (Rignot et al., 2011) and paleo-evidence (Kopp et al., 2009; McKay et al., 2011), we posit that a net mass gain of the AIS appears unlikely and we thus set the lower bound for the AIS contribution in the 21st century to zero.

2.3.3 Bottom-up II: PF08

The third approach considers a higher estimate based on glacio-dynamical constraints (Pfeffer et al., 2008) (PF08). The intervals considered for 21st century contribution to sea-level rise are 16.5–53.8 cm for Greenland and 12.8–62.9 cm for Antarctica (Table 1), which we interpret as uniform distributions. Since the ice-sheet contribution in

¹available for download at http://www.met.rdg.ac.uk/~jonathan/data/ar4_ice_sheet_smb.html

Probabilistic regional sea-level projections

M. Perrette et al.

Title Page

Abstract

Introduction

Conclusions

References

Tables

Figures



Back

Close

Full Screen / Esc

Printer-friendly Version

Interactive Discussion



PF08 was not dependent on a specific temperature change, we also assume independence between the SLR ranges given above and our GMT projections, as well as between both ice sheets. A linear ramping of ice melt over time is assumed, for simplicity.

This scenario is more speculative, especially for AIS, whose ice streams, contrary to GIS's outlet glaciers, are not constrained by bedrock topography (Pfeffer et al., 2008). It is presented here to cover the full range of anticipated 21st century ice-sheet contribution found in the literature to date. Such high estimates are nevertheless not implausible: Rignot and colleagues (2011) have recently shown that continued acceleration of the loss observed between 1992 to 2009 from both ice sheets would raise sea level by approximately 56 cm by 2100 compared to 2009.

2.3.4 Ice-sheet gravitational signature

The AIS and GIS regional fingerprints (Fig. 1c and d) are obtained in a similar manner as the MGIC fingerprint (see Sect. 2.2.2). They take into account the present-day distribution of mass loss as observed from satellite missions (Bamber and Riva, 2010). This spatial distribution of the mass loss region might change in the future, but the influence on sea level patterns is only important in the very near-field of an ice sheet (<1000 km), and is negligible further away for all practical purposes (Bamber and Riva, 2010).

3 Results

3.1 Global-mean contributions

GMT increases over the 21st century are projected to be approximately four times higher under RCP8.5, compared to the lowest scenario, RCP3-PD. In contrast, ocean thermal expansion varies only within a factor of two across the RCPs, from 16 cm (11–23 cm) to 33 cm (23–45 cm) (see Table 1), reflecting the higher thermal inertia of the

Probabilistic regional sea-level projections

M. Perrette et al.

Title Page

Abstract

Introduction

Conclusions

References

Tables

Figures



Back

Close

Full Screen / Esc

Printer-friendly Version

Interactive Discussion



ocean in comparison to the atmosphere. Our global-mean MGIC calculations yield a somewhat narrower range – partly due to the volume area scaling effect – ranging from 12 cm (9–16 cm) for RCP3-PD to approximately 50 % higher projections i.e. 17 cm (13–23 cm), for RCP8.5. The three different sensitivity cases to quantify the contributions from GIS and AIS over the 21st century differ markedly. The upper-bound sensitivity case PF08 suggests a potential contribution of up to 33 cm (21–45 cm) for GIS, and 35 cm (19–51 cm) for AIS. Our top-down sensitivity case yields an estimate which is about a third lower, with a maximum of 27 cm (12–48 cm) for each ice sheet under RCP8.5.

Global mean sea-level projections up to 2050 are relatively independent of the RCP scenarios, and start diverging only in the second half of the 21st century (Fig. 2a). SLR projections under RCP4.5 using various ice-sheet approaches, however, are already on a distinct path by 2025 (Fig. 2b). The PF08 upper-bound stands clearly apart over most of the century because of the idealized, large and constant melting rate.

3.2 Probabilistic coastal projections

A major advance of our Monte Carlo approach is that it enables to compute a probability density function of sea-level change at each grid point (conditionally on the ice-sheet assumptions), combining the uncertainties attached to each individual component (Table 1). The median sea-level pattern is quasi scenario-independent in the top-down case (Figs. 1i–l, and 3a–d), because the ratios of the various SLR contributions are approximately constant across the scenarios (cf. Table 2). The main features are above-average rise at low latitudes, in particular in the Western Pacific and Indian Ocean, and reduced rise at high latitudes. In the IPCC AR4⁺ case (Fig. 3e), the MGIC near the poles compensates for the small ice-sheet contributions in terms of gravity changes, and overcompensates a large dynamic rise in the North Atlantic. The projected SLR pattern is the result of the interplay between steric and mass contributions, and both steric and MGIC terms have strong regional signatures at high latitudes (Fig. 4). In the Northern Hemisphere, particularly in the Northern Atlantic, they act in opposite

Probabilistic regional sea-level projections

M. Perrette et al.

Title Page

Abstract

Introduction

Conclusions

References

Tables

Figures



Back

Close

Full Screen / Esc

Printer-friendly Version

Interactive Discussion



directions: below-average MGIC contributions offset strong dynamic SLR along the East Coast of the USA (Yin et al., 2009). North of 55° N, the sum of mass and steric contributions is below average along all coastlines. At lower latitudes, the deviations from the global mean are smaller but tend to be of the same sign, with an overall above-average SLR (Fig. 4).

In the two approaches where the ice sheets contribute a large fraction to the total SLR, the top-down cases (Fig. 3b–d) and PF08 (Fig. 3f), the uncertainty in the ratio between local and global mean sea level is relatively small, except in the near-field of the ice sheets, or for very large temperature forcing (i.e. RCP8.5, Fig. 3a). These results contrast sharply with the low IPCC AR4⁺ case (Fig. 3e), where ocean dynamics is the main source of spread in projected regional SLR and the uncertainty in the SLR pattern itself may be as large as the uncertainty in the global mean SLR. Across all emission and ice-sheet scenarios, the highest projected coastal SLR occurs near Tokyo with a rise of 10 to 45 % above the global mean (80 % range, Fig. 3a and e, see Fig. S7 in the Supplement for error bars and absolute uncertainty ranges). We find regional variations up to 20 % higher than the mean along the East-Asian coast and in the Indian Ocean, and up to 30 % lower than the mean in mid-latitude Northern America and Europe (30–50° N). Close to the main ice melt sources (Greenland, Arctic Canada, Alaska, Patagonia and Antarctica), crustal uplift and reduced self-attraction cause a below-average rise, and even a sea-level fall in the very near-field of a mass source. Through this mechanism, due to the proximity to the Patagonian and West Antarctic glaciers, high-latitude South America experiences sea-level change up to 30 % below the global mean.

A selection of four world's locations (Fig. 5) shows how the contributions to SLR may vary over space and time. It is noteworthy that land-ice is projected to represent about two third of future SLR in the Bay of Bengal, while its contribution is only about half along the Dutch Coast, mostly due to gravitational effects which practically suppress GIS contribution there. Ocean steric expansion (as the sum of global mean thermal expansion and local dynamic effects) also varies significantly, with 29 cm rise in the

Probabilistic regional sea-level projections

M. Perrette et al.

Title Page

Abstract

Introduction

Conclusions

References

Tables

Figures



Back

Close

Full Screen / Esc

Printer-friendly Version

Interactive Discussion



New York City region and 24 cm rise in the Bay of Bengal, between 1980–1999 and 2090–2099. In this example, the contribution of Glacial Isostatic Adjustment (GIA) was included (based on ICE-5G, VM2, Peltier, 2004) to enable comparison with the other contributions. In New York, which is close to the former Laurentide ice sheet (during the last ice age), it is of the same order of magnitude as other contributions, whereas it is negligible further away (Tokyo and Bay of Bengal). The GIA signal is also negligible along the Dutch coast in our calculations, even though the region is not very distant from the former Fennoscandian ice sheet; however, this value is rather uncertain due to its sensitivity to the adopted ice history and Earth model (Schotman and Vermeersen, 2005). Incidentally, GIA-induced SLR is positive in the chosen locations, but can generally be of both signs (Fig. S8 in the Supplement).

4 Discussion

4.1 Uncertainty characterization

The uncertainty of regional SLR projections in the top-down case, excluding the immediate ice-sheet surroundings, can be up to 35 % greater than the global mean SLR uncertainty (Fig. 6a). The partitioning uncertainty, arising from the prescribed range of 1/3 to 2/3 in the GIS/AIS contributions' ratio, is very large near the ice-sheets, whereas for regions further away (e.g. in the Pacific and Indian Ocean), this uncertainty is only a few centimeters (Fig. 6c) because the GIS and AIS fingerprints have similar magnitudes in these regions (Fig. 1c and d). In other words, the relative contribution of the AIS and GIS will affect local SLR only in the North Atlantic and Southern Ocean. Above-average uncertainty is also found near the Gulf Stream, the Kuroshio current and in the Southern Ocean (Fig. 6b). These regions feature strong sea level gradients governed by ocean dynamics, and while individual GCMs tend to consistently show large changes under climate forcing for these current systems, they often disagree on

Probabilistic regional sea-level projections

M. Perrette et al.

Title Page

Abstract

Introduction

Conclusions

References

Tables

Figures



Back

Close

Full Screen / Esc

Printer-friendly Version

Interactive Discussion



the exact location of the changes as the mean pattern may already present location biases under present-day conditions.

4.2 Comparison to earlier studies

Our projected dynamic changes for the US North-East coast around New York are above the global mean but weaker than in a previous assessment (Yin et al., 2009). This is likely because of large, fine-scale differences in dynamic SLR projected across the continental shelf in this location, which could lead to different interpretation of local SLR (e.g. single grid cells vs. regional average). Additionally, the RCP4.5 scenario implies lower surface warming than the SRES A1B scenario used in earlier work. The projected SLR amplitude also depends on the choice of the members included in the GCM ensemble, whose spatial resolution and skills at reproducing local conditions vary significantly.

Slangen and colleagues (2011) estimated future SLR in the SRES A1B scenario to be globally largest in the NYC region (about 19 cm above the global mean). In their study, however, the main contribution at this location comes from the GIA, which we do not include here (see discussion below and Figs. 5, S8 and S9 in the Supplement). A more detailed comparison of our IPCC AR4⁺ case with Slangen et al.'s (2011) work (Fig. S9 in the Supplement), also including GIA, shows a consistent picture across the two approaches (qualitatively consistent regarding the sign of the regional sea-level departure from the global mean SLR, and quantitatively consistent within the 68 % confidence interval), with largest discrepancies occurring in the nearfield of the large MGIC (e.g. Vancouver). The uncertainty estimates tend to be larger in the present study, due to the different treatment of the uncertainty and in particular due to the broader range of expected 21st century warming in MAGICC6 than in the GCMs selected in Slangen et al. (2011).

Another recent study (Schleussner et al., 2011) projected NYC sea-level rise based on expected AMOC slow-down under future climate forcing, and a transfer function

Probabilistic regional sea-level projections

M. Perrette et al.

Title Page

Abstract

Introduction

Conclusions

References

Tables

Figures



Back

Close

Full Screen / Esc

Printer-friendly Version

Interactive Discussion



between AMOC and SLR obtained from Yin et al. (2009). They obtain a dynamic rise of similar magnitude than the present paper (~10 cm) for the RCP4.5 scenario.

4.3 Sensitivity to distribution of ice mass loss

Densely populated coasts along the Bay of Bengal are projected to experience higher-than-average rise (+10 to +20 %) due to the combined effect of ocean dynamics and gravity changes. This result is sensitive to glacier melt in the Himalayas and other high Asian mountains: if losses of glacial mass are greater than projected, gravitational effects would lower sea-level and compensate for the dynamic rise. This rationale is applicable only if the glacier meltwater actually drains into the ocean, rather than remains on the land near its source (e.g. by filling aquifers). On decadal and longer time scales, we anticipate that glacial meltwater discharge into the oceans will be the dominant process. Similarly to the Bay of Bengal, sea-level around Cape Town rises more than the global mean due to the assumed distribution of ice loss around West Antarctica. A more uniform ice loss over the Antarctic continent would lead to local SLR closer to the global mean (Bamber and Riva, 2010). The details of the mass loss distribution over Greenland have less of an impact except in the very surrounding of the ice sheet (Bamber and Riva, 2010). Other uncertainties include assumptions about solid Earth properties in the generation of our gravitational fingerprints (e.g. the effect of lateral variations in the thickness of the lithosphere is neglected).

4.4 Sensitivity to dynamic ocean SLR pattern scaling

The normalized ocean dynamic patterns explain most of the simulated long-term changes over the course of the 21st century (Figs. S3 and S4 in the Supplement). Our sensitivity tests suggest a small emission scenario dependency of the patterns, in particular for lower emission scenarios. Nonetheless, the inter-scenario range remains significantly smaller than the inter-model range (Figs. S2–S4 in the Supplement). Projections of very large global warming such as in RCP8.5 or peaking scenarios as in

Probabilistic regional sea-level projections

M. Perrette et al.

Title Page

Abstract

Introduction

Conclusions

References

Tables

Figures



Back

Close

Full Screen / Esc

Printer-friendly Version

Interactive Discussion



RCP3PD represent an extrapolation outside of the range of IPCC-AR4 SRES scenarios (A1B, B1 and A2), which are quite similar to each other and do not explore such extreme climate forcing over the next century. Once ensembles of GCM simulations for the new RCP scenarios become available, they can be compared to our SRES-based dynamic sea level projections to verify whether our simple parameterization of dynamic sea-level upon GMT is accurate, or whether more elaborate parameterizations involving other climatic variables are necessary. Despite these potential caveats, the proposed dynamic sea level scaling approach appears to be robust, in an ensemble context, to predict dynamic sea-level change for a range of emission scenarios.

5 Limitations

5.1 Glacial Isostatic Adjustment

In most projections discussed here, sea-level changes associated to the present-day and future GIA in response to previous glaciations were not included, because it is independent from current and projected climatic change. The rate of this process is nearly constant on the time scales considered here (Peltier and Andrews, 1976), albeit with considerable uncertainties. The GIA contribution to global mean SLR is virtually null (Tamisiea, 2011), however, present-day GIA is causing significant sea-level changes in many coastal areas. In particular, close to the former ice-sheets, GIA effects are of the same order of magnitude as the signature of present-day ice loss (Bamber and Riva, 2010; Slangen et al., 2011) (Figs. 5, S8 and S9 in the Supplement). Considering the current limits in models of the earth glacial history and of the GIA process itself, it remains difficult to accurately quantify the uncertainties associated with the available GIA models.

Probabilistic regional sea-level projections

M. Perrette et al.

Title Page

Abstract

Introduction

Conclusions

References

Tables

Figures



Back

Close

Full Screen / Esc

Printer-friendly Version

Interactive Discussion



5.2 Natural variability

In addition to the long-term changes modeled here, interannual to multi-decadal natural variability can significantly influence local sea-level changes. In the Western Pacific, for example, rates of rise between 1993 and 2008 observed by satellite altimetry were twice as large as global mean SLR during the same period (Cazenave and Llovel, 2010).

Past records from tide-gauges suggest that such large deviations from the global mean rise are related to climate indices such as El Niño and the Pacific Decadal Oscillation (Bromirski et al., 2011), and they likely do not reflect a long-term trend during the 20th century. GCMs simulate major modes of natural, interannual variability, but the phase and amplitude generally differs from actual observations, and the response of these modes to climate forcing during the 21st century is even more uncertain (Collins et al., 2010). As a consequence, GCM simulations cannot presently be used to reliably project the future phase of a particular mode of natural variability, or any long-term changes in this mode. Natural-mode variability should however become relatively less significant as the global sea level rises to the higher rates projected here.

5.3 Ice-sheet discharge and ocean freshening

The regional sea level projections described so far do not include the ocean's dynamic response from the additional freshening due to Greenland and Antarctic meltwater discharge (Stammer, 2008), because oceans and ice-sheets were not interactively coupled in the CMIP3 simulations. However, the impact of such coupling is expected to be small over most of the ocean, of the order of a few percent relative to the concurrent global mean rise (Stammer, 2008). More research is needed to address this aspect in detail (Gower, 2010). In particular, a slow-down of the Atlantic Meridional Overturning Circulation (AMOC) in response to Greenland's freshwater forcing may result in enhanced SLR along the North Atlantic coasts (Levermann et al., 2005; Yin et al., 2009) in scenarios with large ice sheet contributions. However, projections of AMOC based on

Probabilistic regional sea-level projections

M. Perrette et al.

Title Page

Abstract

Introduction

Conclusions

References

Tables

Figures



Back

Close

Full Screen / Esc

Printer-friendly Version

Interactive Discussion



an AOGCM ensemble (Schleussner et al., 2011) point toward a dominating influence from increased precipitation and surface air warming over GIS discharge, and suggest that additional ocean freshening coming from the GIS and related AMOC slowdown (up to 10 %, Schleussner et al., 2011) would be less than 5 cm of dynamic SLR in the NYC region.

6 Conclusions

We have derived regional sea-level projections which explore a large range of ice-sheet contributions to sea-level rise during the 21st century. Our method is probabilistic and designed to be flexible with respect to emission scenarios, thanks to an efficient combination of global mean contributions to sea-level change and their regional “fingerprints”. While these fingerprints have previously been described for the non-steric sea level contributions, we have estimated a novel dynamic ocean fingerprint from an ensemble of GCM simulations. This fingerprint is robust across a range of emission scenarios and allows us, in combination with the non-steric fingerprints, to estimate the amplitude as well as the uncertainties of sea level changes along the world’s coastlines. One of the main features of these projections is the robust, above-average rise at low latitudes, especially in the Indian Ocean and Western Pacific, regardless of the assumed ice-sheet loss during the 21st century.

As new component-specific SLR projections become available, our regional sea-level projections can be updated within the presented framework. It is clear that estimating the Greenland and Antarctic ice sheet evolution over the coming century is central to obtaining reliable sea-level rise projections, and process-based estimates of land-ice melt could – and should – eventually replace the estimates of the ice-sheet contributions that are currently available. At this stage, we can only say that the indirect semi-empirical, top-down approach yields significantly higher sea level projections than previously reported (e.g. IPCC-AR4, Meehl et al., 2007a), and we stress that future

Probabilistic regional sea-level projections

M. Perrette et al.

Title Page

Abstract

Introduction

Conclusions

References

Tables

Figures



Back

Close

Full Screen / Esc

Printer-friendly Version

Interactive Discussion



ice-sheet contributions to SLR remain an object of debate (Rahmstorf, 2010; Lowe and Gregory, 2010).

Our projections are readily applicable to impact analysis and adaptation planning, and can be augmented by non-climatic processes such as human-induced modification of land hydrology (Konikow, 2011), local subsidence (e.g. from sediments deposition and groundwater pumping Poland and Davis, 1969) and long-term glacial isostatic adjustment (Peltier and Andrews, 1976). By synthesizing a number of key uncertainties from emission scenarios to regional sea-level changes in a flexible, comprehensive framework, our probabilistic approach and the estimated fingerprints provide important input for impact studies in coastal regions.

Supplementary material related to this article is available online at:
<http://www.earth-syst-dynam-discuss.net/3/357/2012/esdd-3-357-2012-supplement.pdf>.

Acknowledgements. We thank B. Hare, S. Raper, A. Levermann and S. Rahmstorf for discussion and comments on earlier versions of this manuscript, and M. Mengel and J. Gregory for AOGCM diagnostics. We acknowledge the modelling groups, the Program for Climate Model Diagnosis and Intercomparison (PCMDI) and the WCRP's Working Group on Coupled Modelling (WGCM) for their roles in making available the WCRP CMIP3 multi-model data set. Support of this data set is provided by the Office of Science, US Department of Energy. M. P. was supported by the Federal Ministry for the Environment, Nature Conservation and Nuclear Safety (Germany) under the project SURVIVE 11_II_093_Global_A_SIDS_and_LDC. F. W. L.'s work was carried out at the Jet Propulsion Laboratory, California Institute of Technology, under a contract with the National Aeronautics and Space Administration. K. F. and M. M. were supported by the Federal Environment Agency for Germany (UBA) under project UFOPLAN FKZ 370841103.

Probabilistic regional sea-level projections

M. Perrette et al.

Title Page

Abstract

Introduction

Conclusions

References

Tables

Figures



Back

Close

Full Screen / Esc

Printer-friendly Version

Interactive Discussion



References

- Bamber, J. and Riva, R.: The sea level fingerprint of recent ice mass fluxes, *The Cryosphere*, 4, 621–627, doi:10.5194/tc-4-621-2010, 2010. 359, 363, 364, 367, 372, 373
- 5 Bindoff, N. L., Willebrand, J., Artale, V., Cazenave, A., Gregory, J., Gulev, S., Hanawa, K., Le Quéré, C., Levitus, S., Nojiri, Y., Shum, C. K., Talley, L. D., and Unnikrishnan, A.: *Climate Change 2007: The Physical Science Basis, Contribution of Working Group I to the Fourth Assessment Report of the Intergovernmental Panel on Climate Change*, chap. Observations: Oceanic Climate Change and Sea Level, Cambridge University Press, New York City, 2007. 358
- 10 Brohan, P., Kennedy, J. J., Harris, I., Tett, S. F. B., and Jones, P. D.: Uncertainty estimates in regional and global observed temperature changes: A new data set from 1850, *J. Geophys. Res.*, 111, D12106, doi:10.1029/2005JD006548, 2006. 359
- Bromirski, P. D., Miller, A. J., Flick, R. E., and Auad, G.: Dynamical suppression of sea level rise along the Pacific coast of North America: Indications for imminent acceleration, *J. Geophys. Res.*, 116, C07005, doi:10.1029/2010JC006759, 2011. 374
- 15 Cazenave, A. and Llovel, W.: Contemporary Sea Level Rise, *Ann. Rev. Mar. Sci.*, 2, 145–173, 2010. 374
- Chao, B. F., Wu, Y. H., and Li, Y. S.: Impact of artificial reservoir water impoundment on global sea level, *Science*, 320, 212–214, doi:10.1126/science.1154580, 2008. 365
- 20 Church, J. A. and White, N. J.: A 20th century acceleration in global sea-level rise, *Geophys. Res. Lett.*, 33, L01602, doi:10.1029/2005GL024826, 2006. 365
- Clark, J. A. and Lingle, C. S.: Future sea-level changes due to West Antarctic ice sheet fluctuations, *Nature*, 269, 206–209, doi:10.1038/269206a0, 1977. 359
- 25 Collins, M., An, S.-I., Cai, W., Ganachaud, A., Gouilly, E., Jin, F.-F., Jochum, M., Lengaigne, M., Power, S., Timmermann, A., Vecchi, G., and Wittenberg, A.: The impact of global warming on the tropical Pacific Ocean and El Niño, *Nature Geosci.*, 3, 391–397, doi:10.1038/ngeo868, 2010. 374
- Domingues, C. M.: Improved estimates of upper-ocean warming and multi-decadal sea-level rise, *Nature*, 453, 1090–1094, doi:10.1038/nature07080, 2008. 359, 360
- 30 Gower, J. F. R.: Comment on Response of the global ocean to Greenland and Antarctic ice melting by D. Stammer, *J. Geophys. Res.*, 115, C10009, doi:10.1029/2010JC006097, 2010. 374

Probabilistic regional sea-level projections

M. Perrette et al.

Title Page

Abstract

Introduction

Conclusions

References

Tables

Figures



Back

Close

Full Screen / Esc

Printer-friendly Version

Interactive Discussion



Probabilistic regional sea-level projections

M. Perrette et al.

Title Page

Abstract

Introduction

Conclusions

References

Tables

Figures

◀

▶

◀

▶

Back

Close

Full Screen / Esc

Printer-friendly Version

Interactive Discussion



- Gregory, J. M. and Huybrechts, P.: Ice-sheet contributions to future sea-level change, *Philos. T. Roy Soc. A*, 364, 1709–1732, 2006. 358, 366
- Grinsted, A., Moore, J. C., and Jevrejeva, S.: Reconstructing sea level from paleo and projected temperatures 200 to 2100 AD, *Clim. Dynam.*, 34, 461–472, 2009. 365
- 5 Katsman, C. A., Hazeleger, W., Drijfhout, S., van Oldenborgh, G., and Burgers, G.: Climate scenarios of sea level rise for the northeast Atlantic Ocean: a study including the effects of ocean dynamics and gravity changes induced by ice melt, *Climatic Change*, 91, 351–374, doi:10.1007/s10584-008-9442-9, 2008. 359
- Konikow, L. F.: Contribution of global groundwater depletion since 1900 to sea-level rise, *Geophys. Res. Lett.*, 38, 1–5, doi:10.1029/2011GL048604, 2011. 365, 376
- 10 Kopp, R. E., Simons, F. J., Mitrovica, J. X., Maloof, A. C., and Oppenheimer, M.: Probabilistic assessment of sea level during the last interglacial stage, *Nature*, 462, 863–867, doi:10.1038/nature08686, 2009. 366
- Landerer, F. W., Jungclauss, J. H., and Marotzke, J.: Regional Dynamic and Steric Sea Level Change in Response to the IPCC-A1B Scenario, *J. Phys. Oceanogr.*, 37, 296–312, doi:10.1175/JPO3013.1, 2007. 358
- 15 Lemke, P., Ren, J., Alley, R. B., Allison, I., Carrasco, J., Flato, G., Fujii, Y., Kaser, G., Mote, P., and Thomas, R. H.: *Climate Change 2007: The Physical Science Basis, Contribution of Working Group I to the Fourth Assessment Report of the Intergovernmental Panel on Climate Change*, chap. Observations: changes in snow, ice and frozen ground, Cambridge University Press, New York City, 2007. 362
- 20 Levermann, A., Griesel, A., Hofmann, M., Montoya, M., and Rahmstorf, S.: Dynamic sea level changes following changes in the thermohaline circulation, *Clim. Dynam.*, 24, 347–354, doi:10.1007/s00382-004-0505-y, 2005. 374
- 25 Lowe, J. A. and Gregory, J. M.: A sea of uncertainty, *Nat. Reports*, 42–43, doi:10.1038/climate.2010.30, 2010. 358, 364, 365, 376
- McKay, N. P., Overpeck, J. T., and Otto-Bliesner, B. L.: The role of ocean thermal expansion in Last Interglacial sea level rise, *Geophys. Res. Lett.*, 38, L14605, doi:10.1029/2011GL048280, 2011. 366
- 30 Meehl, G. A., Stocker, T. F., Collins, W. D., Friedlingstein, P., Gaye, A. T., Gregory, J. M., Kitoh, A., Knutti, R., Murphy, J. M., Noda, A., Raper, S. C. B., Watterson, I. G., Weaver, A. J., and Zhao, Z.-C.: Global climate projections, in: *Climate Change 2007: The Physical Science Basis. Contribution of Working Group I to the Fourth Assessment Report of the*

Probabilistic regional sea-level projections

M. Perrette et al.

Title Page

Abstract

Introduction

Conclusions

References

Tables

Figures

◀

▶

◀

▶

Back

Close

Full Screen / Esc

Printer-friendly Version

Interactive Discussion



Intergovernmental Panel on Climate Change, edited by: Solomon, S. , Qin, D., Manning, M., Chen, Z., Marquis, M., Averyt, K. B., Tignor, M., and Miller, H. L., Cambridge University Press, Cambridge, UK and New York, NY, USA, 747–845, 2007a. 358, 362, 366, 375

5 Meehl, G. A., Covey, C., Delworth, T., Latif, M., McAvaney, B., Mitchell, J. F. B., Stouffer, R. J., and Taylor, K. E.: The WCRP CMIP3 multimodel dataset, *B. Am. Meteorol. Soc.*, 88, 1383–1394, 2007b. 361

Meinshausen, M., Meinshausen, N., Hare, W., Raper, S. C. B., Frieler, K., Knutti, R., Frame, D. J., and Allen, M. R.: Greenhouse-gas emission targets for limiting global warming to 2 C, *Nature*, 458, 1158–1162, 2009. 360

10 Meinshausen, M., Raper, S. C. B., and Wigley, T. M. L.: Emulating coupled atmosphere-ocean and carbon cycle models with a simpler model, MAGICC6 – Part 1: Model description and calibration, *Atmos. Chem. Phys.*, 11, 1417–1456, doi:10.5194/acp-11-1417-2011, 2011. 359, 360

15 Mitrovica, J. X., Tamisiea, M. E., Davis, J. L., and Milne, G. A.: Recent mass balance of polar ice sheets inferred from patterns of global sea-level change, *Nature*, 409, 1026–1029, doi:10.1038/35059054, 2001. 359

Moss, R. H., Edmonds, J. A., Hibbard, K. A., Manning, M. R., Rose, S. K., van Vuuren, D. P., Carter, T. R., Emori, S., Kainuma, M., Kram, T., Meehl, G. A., Mitchell, J. F. B., Nakicenovic, N., Riahi, K., Smith, S. J., Stouffer, R. J., Thomson, A. M., Weyant, J. P., and Wilbanks, T. J.: The next generation of scenarios for climate change research and assessment, *Nature*, 463, 747–756, doi:10.1038/nature08823, 2010. 359, 360

20 Pardaens, A. K., Gregory, J. M., and Lowe, J. A.: A model study of factors influencing projected changes in regional sea level over the twenty-first century, *Clim. Dynam.*, 36, 2015–2033, doi:10.1007/s00382-009-0738-x, 2010. 359

25 Peltier, W.: Global glacial isostasy and the surface of the ice-age Earth: the ICE-5G (VM2) Model and GRACE, *Annu. Rev. Earth. Planet. Sci.*, 32, 111–149, doi:10.1146/annurev.earth.32.082503.144359, 2004. 370

Peltier, W. R. and Andrews, J. T.: Glacial-Isostatic Adjustment, *The Forward Problem*, *Geophys. J. Roy. Astron. Soc.*, 46, 605–646, doi:10.1111/j.1365-246X.1976.tb01251.x, 1976. 373, 376

30 Pfeffer, W. T., Harper, J. T., and O’Neel, S.: Kinematic constraints on glacier contributions to 21st-century sea-level rise, *Science*, 321, 1340–1343, doi:10.1126/science.1159099, 2008. 366, 367

Probabilistic regional sea-level projections

M. Perrette et al.

Title Page

Abstract

Introduction

Conclusions

References

Tables

Figures

◀

▶

◀

▶

Back

Close

Full Screen / Esc

Printer-friendly Version

Interactive Discussion



- Poland, J. F. and Davis, G. H.: Land subsidence due to withdrawal of fluids, *Rev. Eng. Geol.*, 2, 187–269, 1969. 376
- Radic, V. and Hock, R.: Regionally differentiated contribution of mountain glaciers and ice caps to future sea-level rise, *Nat. Geosci.*, 4, 91–94, doi:10.1038/ngeo1052, 2011. 362, 363
- 5 Rahmstorf, S.: A Semi-Empirical Approach to Projecting Future Sea-Level Rise, *Science*, 315, 368–370, 2007. 365
- Rahmstorf, S.: A new view on sea level rise, *Nature Reports, Climate Change*, 4, 44–45, doi:10.1038/climate.2010.29, 2010. 358, 364, 365, 376
- Rahmstorf, S., Perrette, M., and Vermeer, M.: Testing the robustness of semi-empirical sea level
10 projections, *Clim. Dynam.*, doi:10.1007/s00382-011-1226-7, in press, 2011. 364, 365, 366
- Rignot, E., Velicogna, I., van den Broeke, M. R., Monaghan, A., and Lenaerts, J.: Acceleration of the contribution of the Greenland and Antarctic ice sheets to sea level rise, *Geophys. Res. Lett.*, 38, L05503, doi:10.1029/2011GL046583, 2011. 364, 366, 367
- Schleussner, C. F., Frieler, K., Meinshausen, M., Yin, J., and Levermann, A.: Emulating Atlantic
15 overturning strength for low emission scenarios: consequences for sea-level rise along the North American east coast, *Earth Syst. Dynam.*, 2, 191–200, doi:10.5194/esd-2-191-2011, 2011. 371, 375
- Schotman, H. and Vermeersen, L.: Sensitivity of glacial isostatic adjustment models with shallow low-viscosity earth layers to the ice-load history in relation to the performance of GOCE and GRACE, *Earth Planet. Sc. Lett.*, 236, 828–844, doi:10.1016/j.epsl.2005.04.008, 2005. 370
- 20 Slangen, A. B. A., Katsman, C. A., Wal, R. S. W., Vermeersen, L. L. A., and Riva, R. E. M.: Towards regional projections of twenty-first century, sea-level change based on IPCC SRES scenarios, *Clim. Dynam.*, 38, 1191–1209, doi:10.1007/s00382-011-1057-6, 2011. 359, 371, 373
- 25 Stammer, D.: Response of the global ocean to Greenland and Antarctic ice melting, *J. Geophys. Res.*, 113, C06022, doi:10.1029/2006JC004079, 2008. 374
- Tamisiea, M. E.: Ongoing glacial isostatic contributions to observations of sea level change, *Geophys. J. Int.*, 186, 1036–1044, doi:10.1111/j.1365-246X.2011.05116.x, 2011. 373
- 30 Vermeer, M. and Rahmstorf, S.: Global sea level linked to global temperature, *P. Natl. Acad. Sci. USA*, 106, 21527, doi:10.1073/pnas.0907765106, 2009. 365
- Wigley, T. M. L. and Raper, S. C. B.: Extended scenarios for glacier melt due to anthropogenic forcing, *Geophys. Res. Lett.*, 32, L05704, doi:10.1029/2004GL021238, 2005. 362

Yin, J., Schlesinger, M. E., and Stouffer, R. J.: Model projections of rapid sea-level rise on the northeast coast of the United States, *Nat. Geosci.*, 2, 262–266, doi:10.1038/ngeo462, 2009. 359, 369, 371, 372, 374

5 Yin, J., Griffies, S. M., and Stouffer, R. J.: Spatial Variability of Sea Level Rise in Twenty-First Century Projections, *J. Climate*, 23, 4585–4607, doi:10.1175/2010JCLI3533.1, 2010. 359, 361

ESDD

3, 357–389, 2012

Probabilistic regional sea-level projections

M. Perrette et al.

Title Page

Abstract

Introduction

Conclusions

References

Tables

Figures

⏪

⏩

◀

▶

Back

Close

Full Screen / Esc

Printer-friendly Version

Interactive Discussion



Probabilistic regional sea-level projections

M. Perrette et al.

Table 1. Summary of uncertainty components accounted for in the present study. All uncertainties are combined using Monte Carlo sampling of the parameter distributions and model ensembles (10 000 samples). When not indicated otherwise, the ranges indicate ± 1 s.d.

Component	Description	Range
Temperature and ocean heat uptake	MAGICC ensemble (Bayesian approach)	600 model versions (K and J, respectively)
Global mean thermal expansion	Scaling vs ocean heat uptake	$11.2 \pm 1.2 \times 10^{-23} \text{ mm J}^{-1}$
Dynamic sea level	GCM spatial “fingerprints”	12 fingerprints (mm K^{-1})
Global mean MGIC (Eq. 1)	Global SMB sensitivity b_0	$0.8 \pm 0.2 \text{ mm yr}^{-1} \text{ K}^{-1}$
–	Total volume V_0	$410 \pm 30 \text{ mm}$
–	Pre-industrial temperature T_0 (ref. 1951–1980)	$-0.43 \pm 0.05 \text{ K}$
Ice-sheet: top-down (Eq. 2)	Sea-level sensitivity a	$5.6 \pm 0.4 \text{ mm yr}^{-1} \text{ K}^{-1}$
–	Fast-response term b	$-66 \pm 16 \text{ mm K}^{-1}$
–	Pre-industrial temperature T_0 (ref. 1951–1980)	$-0.43 \pm 0.05 \text{ K}$
–	AIS/GIS partition	1/3–2/3 (uniform)
Ice-sheet: IPCC AR4+	Polynomial fit between temperature and GIS SMB	72 polynomial fits ($\text{mm yr}^{-1} \text{ K}^{-1}$)
Ice-sheet: PF08	AIS	128–629 mm (uniform)
–	GIS	165–538 mm (uniform)

[Title Page](#)
[Abstract](#)
[Introduction](#)
[Conclusions](#)
[References](#)
[Tables](#)
[Figures](#)
[Back](#)
[Close](#)
[Full Screen / Esc](#)
[Printer-friendly Version](#)
[Interactive Discussion](#)


Probabilistic regional sea-level projections

M. Perrette et al.

Table 2. Global mean projected contributions between 1980–1999 and 2090–2099 periods. Ranges are the 16th and 84th percentiles. The unit is centimetre or degree Celsius. All numbers are rounded. Note that mountain glaciers and ice caps (MGIC) include those present at Greenland margins and on the Antarctic Peninsula.

	Thermal expansion (cm)	MGIC (cm)	GIS (cm)	AIS (cm)	Total (cm)	Global mean temperature (°C)
RCP3-PD, top-down	16 (11, 23)	12 (9, 16)	22 (14, 34)*	23 (14, 34)*	75 (59, 95)	1.1 (0.8, 1.4)
RCP4.5, top-down	22 (15, 30)	14 (10, 18)	24 (14, 39)*	24 (13, 38)*	86 (66, 111)	2.0 (1.6, 2.5)
RCP6.0, top-down	24 (16, 33)	14 (10, 19)	23 (12, 37)*	23 (12, 37)*	86 (66, 109)	2.6 (2.1, 3.2)
RCP8.5, top-down	33 (23, 45)	17 (13, 23)	27 (12, 48)*	27 (12, 48)*	106 (78, 143)	4.3 (3.5, 5.5)
RCP4.5, IPCC AR4 ⁺	22 (15, 30)	14 (10, 18)	3 (2, 4)	0 (0, 0)	39 (31, 49)	2.0 (1.6, 2.5)
RCP4.5, PF08	22 (15, 30)	14 (10, 18)	33 (21, 45)	35 (19, 51)	106 (86, 125)	2.0 (1.6, 2.5)

* indicate that ice-sheet contributions are obtained from the top-down approach (see main text).

[Title Page](#)
[Abstract](#)
[Introduction](#)
[Conclusions](#)
[References](#)
[Tables](#)
[Figures](#)
[Back](#)
[Close](#)
[Full Screen / Esc](#)
[Printer-friendly Version](#)
[Interactive Discussion](#)


Probabilistic regional sea-level projections

M. Perrette et al.

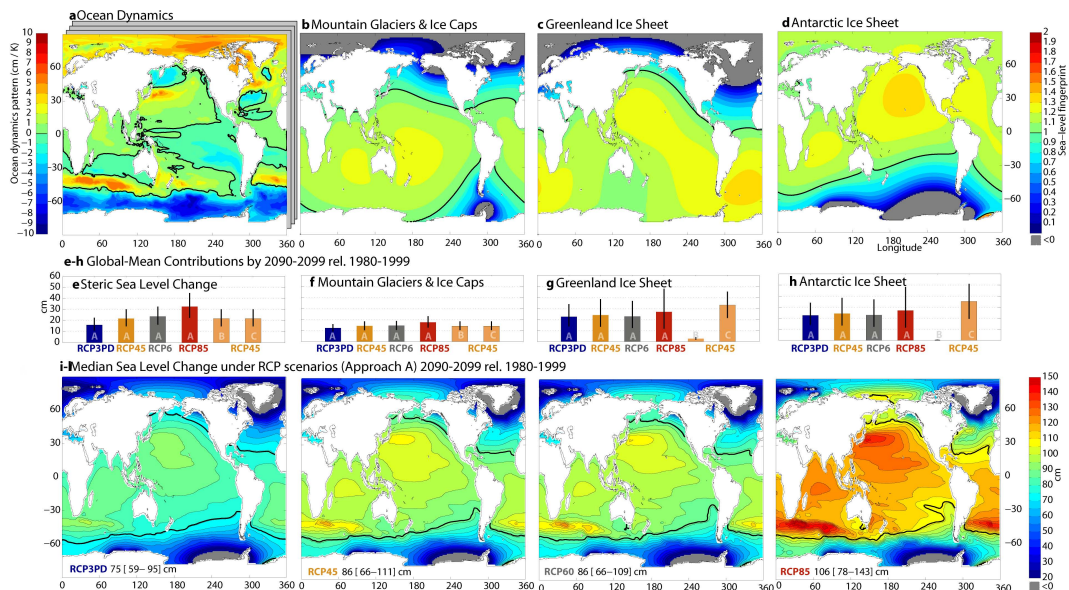


Fig. 1. Sea level fingerprints, their contribution and median 21st century projections **(a)–(l)**. Sea-level fingerprints for ocean dynamics **(a)**, MGIC **(b)**, GIS **(c)** and AIS **(d)**, expressed in unit of regional sea-level rise per unit of global mean temperature change **(a)** or global mean contribution of the source used for scaling **(b–c)**. The temperature-dependent ocean dynamic anomaly pattern is added to global mean thermal expansion **(e)** while mass additions from land-ice are used for the gravitational patterns **(f–h)**. All four boxes are shown for the four RCP scenarios in the top-down approach and only RCP4.5 in the bottom-up cases, indicating median and 68 % uncertainty range. Panels **(i–l)** show projected total SLR for all components combined (contours every 5 cm). The thick black line corresponds to the global mean on all maps, and grey shading indicates areas of sea-level drop.

Title Page

Abstract

Introduction

Conclusions

References

Tables

Figures

◀

▶

◀

▶

Back

Close

Full Screen / Esc

Printer-friendly Version

Interactive Discussion



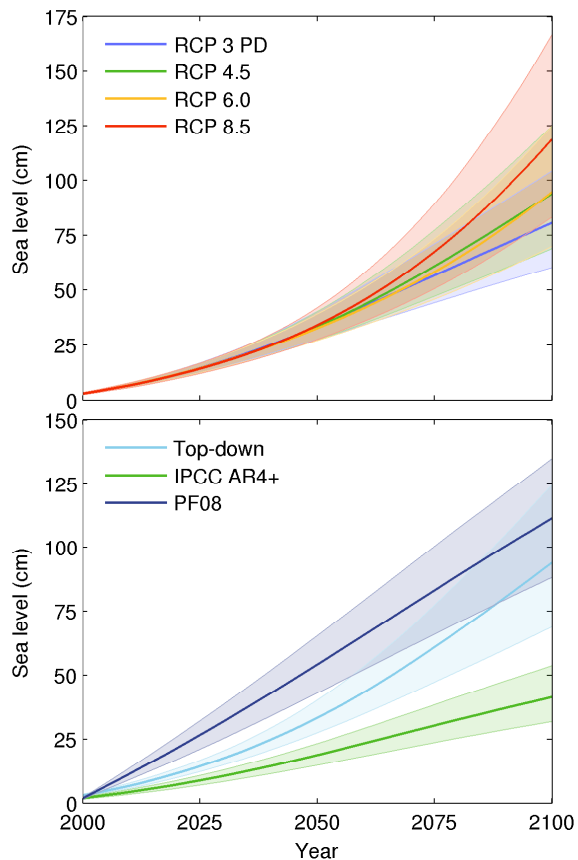


Fig. 2. Projected global mean sea-level rise during the 21st century, for **(a)** the four RCP scenarios in the top-down case and **(b)** the three ice-sheet approaches following the RCP4.5 scenario. The PF08 case is schematically represented as a constant melting rate, as the authors hypothesize an increase of the discharge rate during the first decade, and constant rate afterward.

Probabilistic regional sea-level projections

M. Perrette et al.

Title Page

Abstract

Introduction

Conclusions

References

Tables

Figures

⏪

⏩

◀

▶

Back

Close

Full Screen / Esc

Printer-friendly Version

Interactive Discussion



Probabilistic regional sea-level projections

M. Perrette et al.

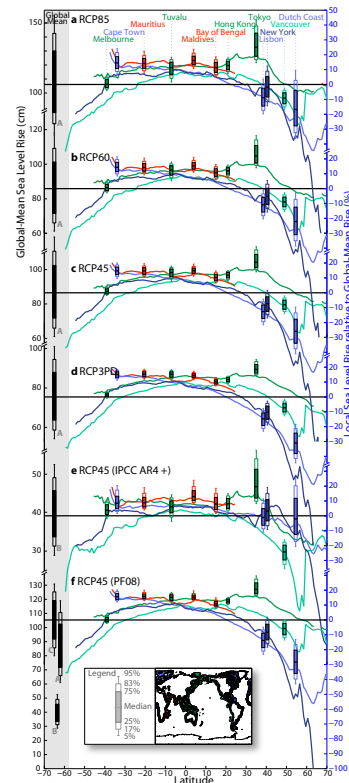


Fig. 3. Projected sea-level rise along world coastlines. Coloured lines show regional sea-level projections, averaged over coastal areas (<300 km from land, including islands) over latitude, and for various oceans (selected coastlines are indicated in the inlet). Global mean SLR (cm) is indicated by a horizontal black bar on the left for each scenario, with error bars indicating 50 %, 68 % and 80 % uncertainty ranges. Particular locations are also shown (averages within 200 km from the black dots on the map, and vertical dashed lines). The uncertainty ranges for these only describe the relative deviation from the global mean (%), to highlight uncertainty in regional fingerprints. The total uncertainty in regional sea-level (shown in Fig. S7 in the Supplement) is a combination of local (right y-axis) and global (left y-axis) sea-level uncertainties.

Title Page

Abstract

Introduction

Conclusions

References

Tables

Figures

◀

▶

◀

▶

Back

Close

Full Screen / Esc

Printer-friendly Version

Interactive Discussion



Probabilistic regional sea-level projections

M. Perrette et al.

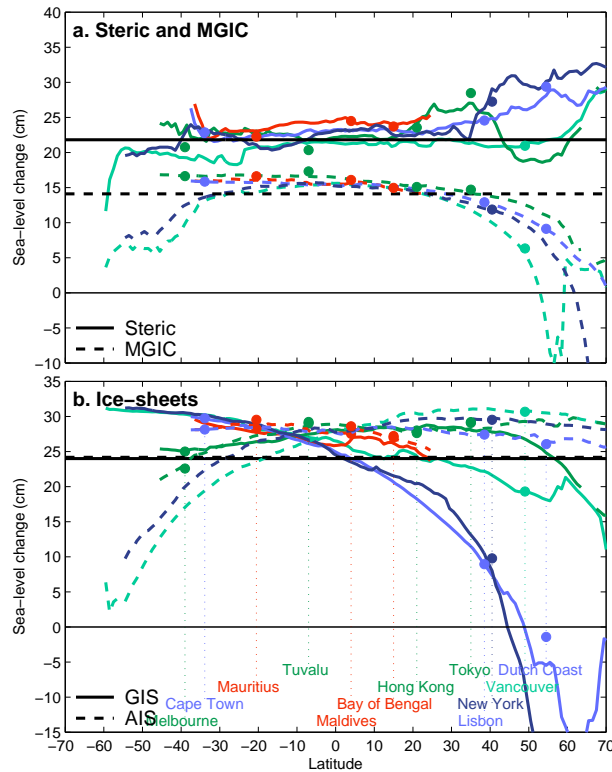


Fig. 4. Projected contributions to sea-level rise along world coastlines. Coloured lines show regional sea-level change due to steric expansion – (a): solid lines, MGIC melt – (a): dashed lines – and ice-sheets wastage (b) (top-down case), averaged over coastal areas, and for various oceans. Global mean contributions (cm) are indicated by a thick horizontal black line (see caption of Fig. 3, in the main text, for more detailed information).

Title Page

Abstract

Introduction

Conclusions

References

Tables

Figures

◀

▶

◀

▶

Back

Close

Full Screen / Esc

Printer-friendly Version

Interactive Discussion



Probabilistic regional sea-level projections

M. Perrette et al.

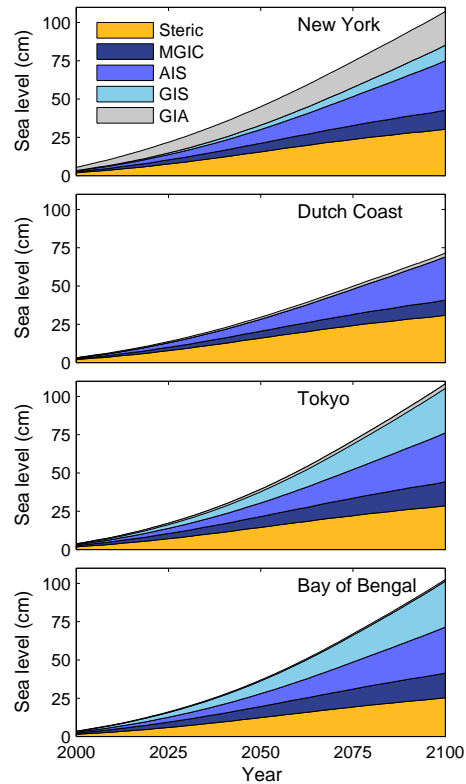


Fig. 5. Projected median contributions to sea-level rise during the 21st century, around four coastal locations. Each color represents a contribution to sea-level rise. In this example, the glacial isostatic adjustment (GIA) contribution (based on ICE-5G, VM2) has been included for comparison with the other contributions.

[Title Page](#)
[Abstract](#)
[Introduction](#)
[Conclusions](#)
[References](#)
[Tables](#)
[Figures](#)
[◀](#)
[▶](#)
[◀](#)
[▶](#)
[Back](#)
[Close](#)
[Full Screen / Esc](#)
[Printer-friendly Version](#)
[Interactive Discussion](#)


Probabilistic regional sea-level projections

M. Perrette et al.

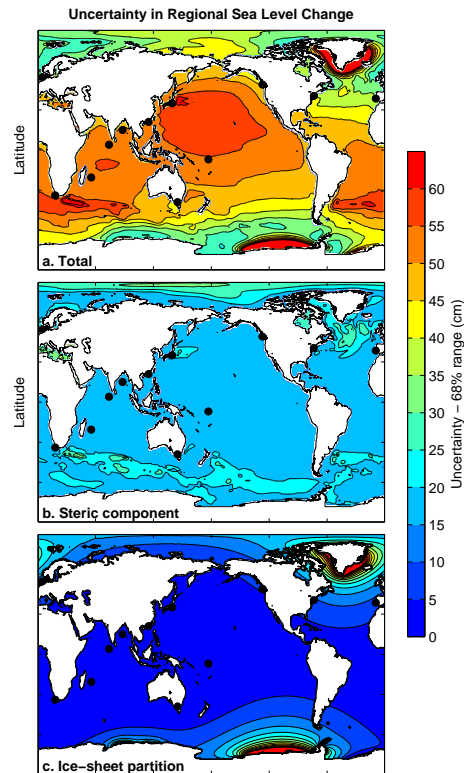


Fig. 6. Uncertainty in regional sea level change **(a)–(c)**. Uncertainty (68% range) in sea-level change **(a)** and its steric component **(b)**, for the RCP4.5 scenario in the top-down case. The uncertainty resulting from GIS/AIS partition in the top-down approach is illustrated in panel **(c)**, for a total ice-sheet contribution equal to the ensemble median. Contours lines indicate 5-cm intervals. Black dots indicate individual locations highlighted in Fig. 3.

Title Page

Abstract

Introduction

Conclusions

References

Tables

Figures

◀

▶

◀

▶

Back

Close

Full Screen / Esc

Printer-friendly Version

Interactive Discussion

